Functional Evidence of Pulmonary Extracellular Vesicles in Infectious and Noninfectious Lung Inflammation

Heedoo Lee,* Duo Zhang,* Debra L. Laskin,† and Yang Jin*

Acute lung injury (ALI)/acute respiratory distress syndrome (ARDS) is a highly complex process that can be triggered by both noninfectious (sterile) and infectious stimuli. Inflammatory lung responses are one of the key features in the pathogenesis of this devastating syndrome. How ALI/ARDS-associated inflammation develops remains incompletely understood, particularly after exposure to sterile stimuli. Emerging evidence suggests that extracellular vesicles (EVs) regulate intercellular communication and inflammatory responses in various diseases. In this study, we characterized the generation and function of pulmonary EVs in the setting of ALI/ARDS, induced by sterile stimuli (oxidative stress or acid aspiration) and infection (LPS/Gram-negative bacteria) in mice. EVs detected in bronchoalveolar lavage fluid (BALF) were markedly increased after exposure of animals to both types of stimuli. After sterile stimuli, alveolar type-I epithelial cells were the main source of the BALF EVs. In contrast, infectious stimuli–induced BALF EVs were mainly derived from alveolar macrophages (AMs). Functionally, BALF EVs generated in both the noninfectious and infectious ALI models promoted the recruitment of macrophages in in vivo mouse models. Furthermore, BALF EVs differentially regulated AM production of cytokines and inflammatory mediators, as well as TLR expression in AMs in vivo. Regardless of their origin, BALF EVs contributed significantly to the development of lung inflammation in both the sterile and infectious ALI. Collectively, our results provide novel insights into the mechanisms by which EVs regulate the development of lung inflammation in response to diverse stimuli, potentially providing novel therapeutic and diagnostic targets for ALI/ARDS. ***The Journal of Immunology*****, 2018, 201: 1500–1509.**

Accumulating data have demonstrated that extracellular vesicles (EVs) regulate diverse cellular and biological processes related to human diseases, via facilitating intercellular cross-talk (1). EV-like molecules were initially described by Chargaff and West (2) as platelet-derived particles found in plasma. Subsequently, EVs have been isolated from most cell types and biological fluids including bronchoalveolar lavage fluid (BALF) (3, 4). The discovery of EVs in BALF offers a novel insight into lung physiology and the pathogenesis of human lung diseases.

EVs are highly heterogeneous, varying in size, composition, and amounts generated; this is largely based on their origin and the environmental stimuli that induce their production. Accumulation of EVs in tissues is a dynamic process, constantly changing depending on the activation state of cells producing them and the tissue microenvironment, after exposure to noxious stimuli. The International Society of Extracellular Vesicles has defined three main subgroups of EVs based on size, composition, and mechanisms of formation (5, 6); these are exosomes (Exos), microvesicles (MVs), and apoptotic bodies (ABs). Exos are the smallest subgroup of EVs measuring ∼30–100 nm in diameter. Exos' generation is closely related and dynamically associated with endosomes/lysosomes, the *trans*-Golgi network, and multivesicular bodies (7, 8). Exos are released from cells after multivesicular bodies fuse with the plasma membrane (8). The second group of EVs are MVs that protrude from plasma membranes (9). Their biogenesis involves the outward budding and expulsion of plasma membrane from the cell surface resulting in the formation of small vesicles with sizes ranging from 100 nm to 1 μm (9). MVs are generated via the dynamic interplay between phospholipid redistribution and cytoskeletal protein contraction. This process, which is energy dependent and requires ATP, is triggered by translocation of phosphatidylserine to the outer-membrane leaflet through amino-phospholipid translocase activity (10, 11). In contrast to Exos and MVs, which are released from healthy cells and play an important role in cell communication, the third group of EVs, ABs, are formed during the process of apoptosis. ABs are the largest of the EVs, at roughly 1000–2000 nm in diameter, they are comparable in size to platelets (12).

MVs and Exos carry a variety of components, including RNAs and proteins. Some of the proteins have been used as markers for EVs. Because these proteins are also expressed on cells generating EVs, they provide information about their origin (13). Common marker proteins include: tetraspanins such as CD9, CD63, CD81, and CD82; 14-3-3 proteins, MHC molecules, and cytosolic proteins such as heat shock proteins; Tsg101 and the Endosomal Sorting Complex Required for Transport (ESCRT-3)–binding

*Division of Pulmonary and Critical Care Medicine, Department of Medicine, Boston University, Boston, MA 02118; and †Department of Pharmacology and Toxicology, Ernest Mario School of Pharmacy, Rutgers University, Piscataway, NJ 08854

ORCIDs: 0000-0002-2168-3643 (H.L.); 0000-0003-0361-4174 (D.Z.).

Received for publication February 26, 2018. Accepted for publication June 25, 2018.

This work was supported by National Instiutes of Health (NIH) Grants R01HL102076, R21AI121644, R33 AI121644, R01GM111313, and R01GM127596, a Boston University School of Medicine Wing Tat Lee award (to Y.J.), and NIH Grants ES004738, AR055073, and ES005022 (to D.L.L.).

Address correspondence and reprint requests to Dr. Yang Jin, Division of Pulmonary and Critical Care Medicine, Department of Medicine, Boston University, 72 East Concord Street, Boston, MA 02118. E-mail address: yjin1@bu.edu

The online version of this article contains supplemental material.

Abbreviations used in this article: AB, apoptotic body; Acid-EV, BALF EV obtained from mouse exposed to acid inhalation; AECI, type I alveolar epithelial cell; ALI, acute lung injury; AM, alveolar macrophage; ARDS, acute respiratory distress syndrome; Bac (G^-)–EV, BALF EV obtained from mouse exposed to gram-negative bacteria; Bac (G^+)–EV, BALF EV obtained from mouse exposed to gram-positive bacteria; BALF, bronchoalveolar lavage fluid; Con-EV, BALF EV obtained from mouse exposed to control; DLS, dynamic light scattering; EV, extracellular vesicle; Exos, exosome; Hyp-EV, BALF EV obtained from mouse exposed to hyperoxia; LPS-EV, BALF EV obtained from mouse exposed to LPS; miRNA, microRNA; MV, microvesicle; NTA, nanoparticle tracking analysis; OMP, outer membrane protein; OMV, outer membrane vesicle; qPCR, quantitative PCR; TEM, transmission electron microscopy; WT, wild type.

protein Alix (7). However, these proteins are not specific to either MVs or Exos. Moreover, no single marker can uniquely identify a subgroup of EVs.

In humans, acute lung injury (ALI)/acute respiratory distress syndrome (ARDS) can develop as a consequence of exposure to infectious pathogens or to noninfectious noxious stimuli. Although noninfectious or sterile pathology is modeled experimentally by hypoxia, acid inhalation, and ventilator-induced baro-trauma (14), infection-induced ALI/ARDS is induced by bacteria or viruses, or various components of these agents, such as LPS or lipoteichoic acid. Earlier studies suggested an association between ALI and the generation of microparticles (MPs) derived from platelets, neutrophils, monocytes, lymphocytes, RBCs, endothelial cells, and epithelial cells (15). Although initially termed MPs, it is now recognized that these are, in fact, MVs. However, the function of these MVs remains undetermined. Numerous cell types reside within the lung, including macrophages and epithelial cells, which play an important role in host defense against inhaled environmental toxins and microorganisms. How these cells communicate is unknown. We speculate that MVs play a key role in this activity, and the present studies are designed to test this hypothesis using different models of ALI. We found that EVs are released into BALF in both sterile and infectious mouse models of ALI; however, there were significant differences in the function of the EVs generated in the different ALI models. These studies provide novel insights on the role of EVs in lung disease pathogenesis in vivo. This may lead to the development of novel therapeutics for the treatment of ALI induced by sterile or infectious stimuli.

Materials and Methods

Materials

PE-conjugated anti–pan cytokeratin Ab (ab52460) and anti–*Pseudomonas aeruginosa* outer membrane protein (OMP) Ab [B11] (ab35835) were purchased from Abcam (Cambridge, MA). PE-conjugated anti–Ly-6G Ab was purchased from eBioscience (San Diego, CA). Anti-CD31, anti-CD68, and anti-CD9 Abs were from Santa Cruz Biotechnology (Santa Cruz, CA).

Animals

Wild type (WT) C57BL/6 mice (6–8 wk of age) were obtained from The Jackson Laboratory (Bar Harbor, ME). All animal protocols were approved by the Boston University Institutional Animal Care and Use Committee. All experimental protocols and methods were approved by Boston University and were carried out in accordance with the approved guidelines.

Bacteria culture

Pseudomonas pneumoniae (P. pneumoniae) PA103 were cultured overnight in Luria-Bertani medium at 37˚C in a rotator at 250 rpm. For *Streptococcus pneumoniae (S. pneumoniae)* (6303; American Type Culture Collection) culture, after overnight incubation on 5% sheep blood agar plates (BD Biosciences), freshly grown colonies were suspended in Brain Heart Infusion Broth medium (Sigma-Aldrich, St. Louis, MO) and incubated for 2 h at 37˚C. Bacterial concentrations were assessed by serial dilutions using OD600 and were diluted to final CFU concentrations as needed for each experiment.

Cell culture

Lung epithelial E10 cells (16) and alveolar MH-S macrophages (CRL-2019; American Type Culture Collection) were maintained in DMEM or RPMI-1640 with 10% FBS and 1% penicillin/streptomycin. Cells were cultured at 37˚C in a humidified atmosphere with 5% CO_2 and 95% air. For hyperoxia exposure, cells were exposed to 95% oxygen/5% CO_2 in modular exposure chambers, as previously described (17). For bacterial infections, cells were infected with *P. pneumonia* or *S. pneumonia*, as described previously (18, 19). Briefly, cells were incubated with bacteria (10^6 CFU) for 4 h, followed by extensive washing with PBS containing 2% penicillin-streptomycin. The cells were then incubated with DMEM containing 2% penicillin-streptomycin for 24 h. The culture media was collected and centrifuged, and EVs were isolated from the supernatants. Protein concentrations were measured using the Bradford assay. Residual bacteria in supernatants were analyzed by measuring OD600 after overnight incubation of the samples at 37˚C; none were detected.

ALI models

For hyperoxia-induced ALI, mice were exposed to 100% oxygen in modular exposure chambers, as previously described (20). For generating acid-, LPS-, and bacteria-induced ALI, hydrochloric acid (0.1 N, [pH 1.5]), LPS (1 μg/mouse), or live bacteria (10^6 CFU) (21) were instilled intratracheally into the mouse lung, respectively. At the designated time points after administration, mice were euthanized and BALF was collected. The methods are summarized in Table I.

EV isolation from BALF and cell-cultured medium

Previously reported protocols were used to isolate MVs, Exos, and ABs (3, 12, 22). Briefly, BALF or cell-cultured medium was centrifuged at 300 × *g* for 5 min to eliminate inflammatory or dead cells. The supernatant was then collected and centrifuged at 2000 × *g* for 10 min to pellet ABs (12). To isolate MVs, the AB-depleted supernatant was passed through a filter with a 0.45-μm pore size to completely remove the instilled bacteria from the samples. The filter was then washed twice with cold PBS to completely recover the MVs, followed by centrifugation at 16,000 × *g* for 40 min (23, 24). The MVs obtained fell into the size range of 100–400 nm. We found that the filtration step had no effect on the amount of recovered MVs or on their size distribution (data not shown). The resulting supernatant was ultracentrifuged at 100,000 × *g* for 1 h to pellet Exos (25). The same EV isolation procedure was used for all ALI models. Isolated vesicles were resuspended in cold PBS and analyzed using a dynamic light scattering (DLS) instrument (Brookhaven 90plus Nano-particle Sizer), NanoSight (Malvern, U.K.), and transmission electron microscopy (TEM). The purity of the isolated EVs were confirmed by Western blotting with Abs against EV markers (CD63 and TSG101) and DAMP proteins (HMGB1 and S100A4), which were not detectable in the purified EVs (Supplemental Fig. 1A).

Nanoparticle tracking analysis

To determine the size and concentration of EVs nanoparticle tracking analysis (NTA) was performed at the Nanomedicines Characterization Core Facility (The University of North Carolina at Chapel Hill, Chapel Hill, NC). Briefly, isolated EV samples were water-bath sonicated to help dispel aggregates and diluted to a concentration between 1×10^8 and 5×10^8 particles/ml in filtered PBS, in a final volume of 1 ml. The samples were then analyzed using NanoSight NS500 (NanoSight; Malvern Instruments) to capture particles in Brownian motion. The hydrodynamic diameters were calculated using the Stokes-Einstein equation. The 100 nm standard particles and the diluent PBS alone were used for reference. Three independent experiments were conducted, and each sample was analyzed three to four times to obtain average value. Camera level and threshold are set as high and low, respectively, as needed to see all particles in a sample without creating noise. We used the same NTA settings for all the samples (camera type: scientific CMOS; camera level: 16; and detection threshold: 5).

Flow cytometry

Flow cytometric analysis of BALF EVs was performed as described previously with minor modifications (25). Isolated EVs were coupled to equal amounts (10 μl) of aldehyde/sulfate latex beads (Thermo Fisher Scientific, Rockford, IL) for 2 h, and the EV-coated beads were blocked with 4% BSA for 1 h. The bead-bound EVs were then permeabilized and fixed for 5 min with 0.2% Triton X-100 and 2% formaldehyde, followed by incubation with designated Abs. For detection of lung epithelial EVs, anti–pan cytokeratin, anti-PDPN, and anti-SPC Abs (26) were used. For detection of alveolar macrophage (AM) EVs, anti-CD68 Ab (27) was used. For detection of endothelial and PMN-derived EVs, anti-CD31 and anti–Ly-6G Ab were used, respectively. Based on the negative control (noncoated beads), positive EV-bead particles were counted in each sample. Flow cytometry analysis was performed using a FACSCalibur instrument (BD Biosciences) and the data were analyzed using FlowJo software (Tree Star, San Carlos, CA).

Differential inflammatory cell counts in BALF

Cell counting for AMs and neutrophils in mouse BALF was conducted as described previously (28). For cytospin preparations, cell suspension was cytocentrifuged at 300 × *g* for 5 min using a Shandon Cytospin 4 (Thermo Fisher Scientific). Slides were air-dried and stained with Hema 3 Fixative and Solutions (PROTOCOL). Differential cell counts were evaluated under a light microscope.

Table I. Techniques for generation of various ALI models

ALI Models	Technique	Period (d)
Hyperoxia	100% oxygen exposure in modular chambers	3
Acid	0.1 N HCl aspiration (50 μl/mouse)	1
LPS	50 μl saline containing 1 μg LPS	1
Live bacteria	50 μl saline containing 10^6 CFU (*P. pneumoniae* or *S. pneumoniae*)	1

ELISA

Mouse BALF was collected 24 h after EV instillation and centrifuged at 300 × *g* for 5 min to get rid of inflammatory cells. TNF, IL-1β, IL-6, IL-10, IL-21, and MIP2 levels in the BALFs were then analyzed using DuoSet ELISA Development Systems (R&D Systems), according to the manufacturer's recommendation.

Mouse mTOR signaling PCR array

BALF inflammatory cells were isolated from the EV-instilled mice (n = 4 per group) and incubated on cell culture plates for 20 min to allow adhesion of AMs (29). Total RNA was then isolated from the adhered AMs using miRNeasy Mini Kits (Qiagen), and cDNAs were generated using Reverse Transcription Kit (Thermo Fisher Scientific). Mouse mTOR signaling profiles were then analyzed using the RT^2 Profiler PCR Array System (Qiagen).

Real-time quantitative PCR

Total RNAs were purified from the isolated BALF macrophages using miRNeasy Mini Kits (Qiagen). Purified RNA concentration was measured using the NanoDrop Lite Spectrophotometer (Thermo Fisher Scientific), followed by reverse transcription to generate cDNAs. SYBR Green–based real-time quantitative PCR (qPCR) was performed to detect specific mRNAs. For relative expression levels of mRNAs, the β-actin level was used as a reference housekeeping gene. The sequences of primers are shown in Table II.

Statistical analysis

For all experiments, the exact n values and statistical significances were shown in the corresponding figure and figure legends. Representative data from identical results are shown. Statistical analysis was performed with unpaired two-tailed Student t test and one-way ANOVA. The p values < 0.05 were considered statistically significant ($^*p < 0.05$, $^{**}p < 0.01$, $^{***}p < 0.001$, $^{\#}p < 0.05$, $^{\#\#}p < 0.01$, and $^{\#\#\#}p < 0.001$).

Results

EVs are differentially induced and detected in BALF, in response to sterile or infectious stimuli

Both sterile and infectious stimuli–induced ALI models have been established in the past decades (14). We selected four well-established ALI mouse models to investigate EV generation, as detailed in Table I. Hyperoxia (oxidative stress) and acid exposure represent sterile or noninfectious stimuli–induced lung injury, whereas LPS and live–*P. pneumoniae* instillation reflect the infectious lung injury model (Table I). We first isolated the three types of EVs (AB, MV, and Exos) from mouse BALF using sequential centrifugation and size filtration, as described previously (3, 30, 31). Sizes and morphology of the EVs were initially analyzed using DLS (Fig. 1A), NTA (Fig. 1B), and TEM (Fig. 1C). The size ranges of the isolated ABs, MVs, and Exos were 1000–3000, 150–500, and 50–200 nm, respectively (Fig. 1A–C). EV amount was also determined using EV proteins, as shown in Fig. 1D. Approximately 60% of BALF EVs fell into the range of MVs, 21% were Exos and approximately 19% were ABs. Interestingly, the generation of BALF EVs was significantly upregulated in both noninfectious (Fig. 1E) and infectious ALI models (Fig. 1F). Moreover, MVs were the most robustly induced type of EVs in BALF obtained from both the sterile stimuli (hyperoxia or acid) and infectious stimuli (LPS or live Gram-negative (G^-) bacteria, *P. pneumoniae*) models

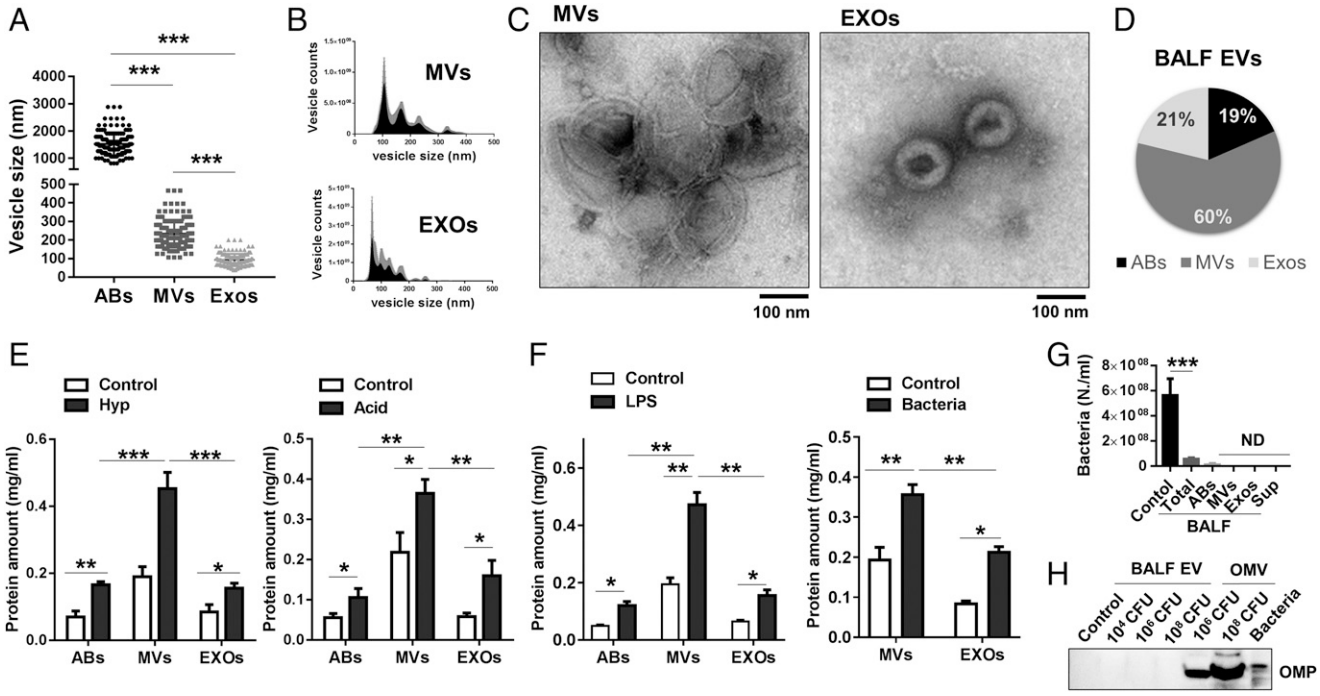

FIGURE 1. Generation of BALF EVs from noninfectious and infectious stimuli–induced ALI models. (**A**–**D**) Three subpopulations of EVs (ABs, MVs, and Exos) were isolated from mouse BALF. The vesicle size and morphology were analyzed using DLS (A), NTA (B), and TEM (C). Pie graphs indicate the average percentages of each type of EV protein (D) (n = 3 mice per group). (**E** and **F**) Three types of EVs were isolated from mouse BALF after sterile stimuli exposure (3 d of hyperoxia and 1 d of acid) (E) or infectious stimuli (1 d of LPS and *P. pneumoniae*) (F), followed by measuring protein concentrations of the isolated EVs. (F and **G**) BALFs were collected from *P. pneumoniae*–exposed mice, followed by sequential isolation of the indicated EVs. The bacteria growth was measured using OD600 nm (G). Bacteria OMP was determined using Western blotting (**H**). The same number of live bacteria was used as positive controls. (mean ± SD, n = 3–4 mice per group). $^*p < 0.05$, $^{**}p < 0.01$, and $^{***}p < 0.001$ between the groups indicated.

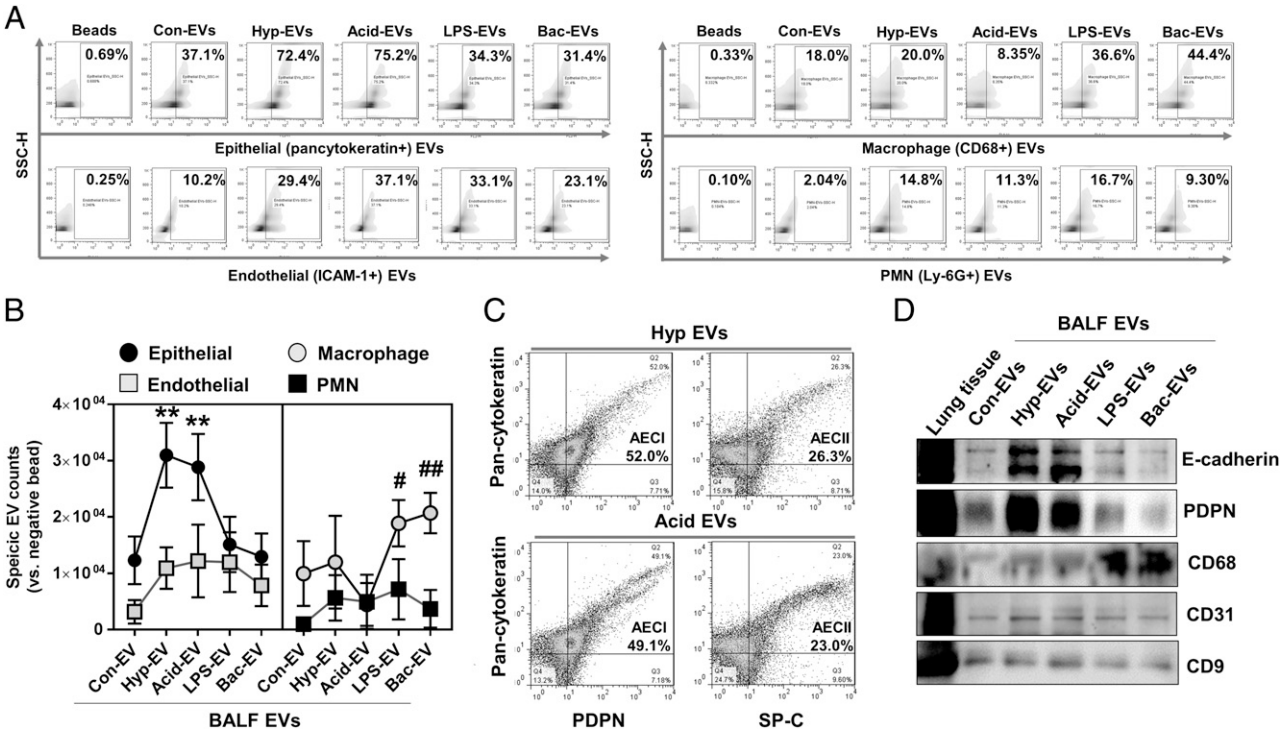

FIGURE 2. Determination of the origin of BALF EVs derived from noninfectious or infectious ALI models. (**A**–**C**) BALF EVs (containing MVs and Exos) were isolated from mice that were exposed to hyperoxia, acid, LPS, or *P. pneumoniae*, followed by FACS analysis of the EVs, as described in *Materials and Methods*. The populations of cell type–specific EVs in response to different stimuli are shown (A and B). PDPN- (AECI marker) and SP-C–positive (type II alveolar epithelial cell marker) EVs were detected in the total BALF EVs derived from noninfectious ALIs (C) (mean ± SD, $n = 3$–4 mice per group). (**D**) Western blot analysis of the BALF EVs from the ALI models using the indicated Abs (representative data, $n = 3$). $^{**}p < 0.01$, $^{\#}p < 0.05$, $^{\#\#}p < 0.01$ versus control EVs.

(Fig. 1E, 1F). Given that bacteria also release outer membrane vesicles (OMVs), which are in the same size range with Exos (32), we next determined whether the BALF EVs isolated after *P. pneumoniae* contain any bacterial OMVs. Previous reports showed a rapid clearance of bacteria from the lung (33, 34). For example, live bacteria remaining in the lung at 4 h after bacterial instillation is ∼7.3% (*S. pneumoniae*) and 13% (*P. pneumoniae*) (33). Therefore, to prevent mixing with OMVs, we isolated the EVs at 24 h after bacterial instillation from the BALF. To further determine whether the isolated BALF EVs were originated from host cells, we first confirmed a significant reduction of the live bacteria in the BALF (Fig. 1G). Additionally, neither bacteria nor bacterial OMP was detected in the purified EVs (MVs plus Exos) (Fig. 1G, 1H).

Determine the cellular origin of BALF EVs after sterile or infectious stimuli

EVs often carry the same markers as their "mother" cells (13). Therefore, we used the specific cell type markers to determine the origin of BALF EVs. Because we were not focused on Abs, in all subsequent studies, BALF EVs refer to MVs and/or Exos. We found that the epithelial marker–positive BALF EVs dramatically increased after noninfectious stimuli (hyperoxia and acid exposure) (Fig. 2A, 2B). In contrast, EVs carrying macrophage markers were highly upregulated after LPS or *P. pneumoniae* exposure (Fig. 2A, 2B). Additionally, EVs carrying endothelial cell markers and PMN markers were mildly induced after stimuli (Fig. 2A, 2B). PDPN and SP-C are specific markers for type I alveolar epithelial cell (AECI) and type II alveolar epithelial cell, respectively (26). As shown in Fig. 2C, the majority of epithelial EVs were derived from the PDPN-positive AECI. We confirmed these observations using Western blot analysis (Fig. 2D). Both common epithelial markers (E-cadherin) and AECI (PDPN) markers were highly expressed in the EVs induced by hyperoxia and acid exposure. In contrast, the macrophage marker CD68 was strongly increased in EVs induced by LPS or *P. pneumoniae* (Fig. 2D). As expected, endothelial markers (CD31) in BALF EVs were unchanged by either sterile (hyperoxia or acid) or infectious (LPS or bacteria) stimuli.

BALF EVs induced by sterile or infectious stimuli promote inflammatory lung responses

To investigate the functional significance of BALF EVs in the development of ALI, we performed the following experiments: First, we isolated BALF EVs (MVs plus Exos) from mice treated with noninfectious or infectious stimuli. The BALF EVs were then instilled intratracheally into the lungs of healthy mice, as illustrated in Fig. 3A. Efficient uptake of the exogenously delivered BALF EVs by AMs was confirmed (Fig. 3B). In this study, we refer to BALF EVs that were obtained from the mice exposed to control, hyperoxia, acid inhalation, LPS, or gram-negative bacteria [Con-EVs, Hyp-EVs, Acid-EVs, LPS-EVs, or Bac (G^-)–EVs, respectively]. BALF EVs obtained from the mice exposed to either sterile or infectious stimuli strikingly triggered the recruitment of macrophages to the lung. In contrast, we did not observe macrophage recruitment in mice receiving Con-EVs from control mice (Fig. 3C, 3D). Furthermore, in mice treated with the Hyp-EVs, Acid-EVs, LPS-EVs, or Bac (G^-)–EVs, a variety of inflammatory cytokines were significantly increased in BALF (Fig. 3E). We also found that EV-containing cytokines were negligible when compared with EV-induced cytokines in vivo, indicating that the EV-induced cytokines did not come from the instilled EVs (Supplemental Fig. 1B). Notably, neutrophil infiltration and MIP2 chemokine induction, two key factors for PMN recruitment (35), were only observed after instillation of Bac (G^-)–EVs, suggesting an LPS-independent pathway (Fig. 3C, 3E).

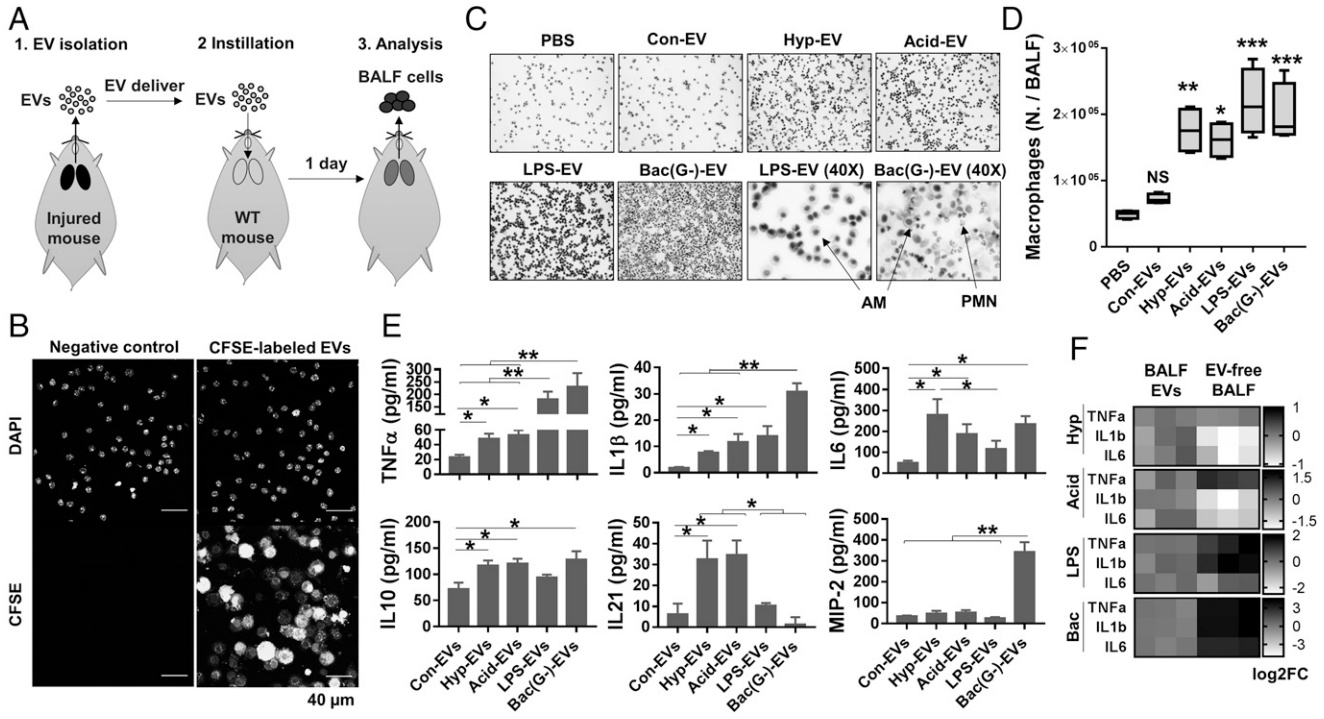

FIGURE 3. Effects of the BALF EVs derived from various ALI models on macrophage recruitment and lung inflammation. (**A**–**E**) BALF EVs were isolated from various ALI (hyperoxia, acid, LPS, or Gram-negative *P. pneumoniae*) models. CFSE-labeled BALF EVs were intratracheally delivered into WT mouse lung (20 μg of EVs per mouse), as illustrated in (A). One day after instillation of the EVs, the BALF cells were isolated from the recipient mouse, followed by tracking of CFSE EVs using confocal microscopy (B) or H&E staining of isolated inflammatory cells (C). AM count is shown in (D) (box and whisker plot, $n = 4$ mice per group). Levels of inflammatory cytokines and MIP2 chemokine in the BALFs were measured using ELISA (E) (mean ± SD, $n = 3$ mice per group). (**F**) Isolated BALF EVs or EV-free BALFs were instratracheally instilled into mouse lung. One day later, AMs were collected, and inflammatory genes were analyzed using qPCR (heat map, $n = 3$ mice per group). $^{*}p < 0.05$, $^{**}p < 0.01$, and $^{***}p < 0.001$ versus control EVs or between the groups indicated.

In further studies, we compared the effects of EV-free BALF with BALF containing EVs on the development inflammatory lung responses in vivo. As shown in Fig. 3F, EV-free BALF obtained from the infectious ALI models highly augmented proinflammatory cytokine gene expression, indicating a significant contribution of BALF soluble factors (non–EV-cargo) to the development of infectious lung inflammation. Conversely, cytokine gene expression after treatment of mice with EV-free BALF from sterile ALI models were less effective in inducing gene expression than sterile ALI–associated BALF EVs. These data indicate that both BALF EVs and BALF soluble factors contribute to the development of lung inflammation in ALI/ARDS. However, EVs play a dominant role in the development of sterile inflammation, whereas soluble factors are more predominant in the infectious inflammatory responses.

Noninfectious and infectious stimuli–induced BALF EVs differentially alter gene expression of inflammatory signaling molecules in AMs

AMs are the first defense against noxious stimuli and the main immune cell type in the lung (36). We next explored inflammatory gene expression in mouse AMs after exposure to the Con-EVs, Hyp-EVs, Acid-EVs, LPS-EVs, Bac (G^-)–EVs, or BALF EV obtained from mice exposed to gram-positive bacteria [Bac (G^+)–EVs]. As described above, WT mice were first treated with BALF EVs isolated from noninfectious or infectious stimuli–treated mice. In these studies, each recipient mouse received BALF EVs obtained from one donor mouse via intratracheal instillation. After 24 h, AMs were collected from recipient mice. Initially, we analyzed TLR signaling pathway–related genes in AMs. As shown in Fig. 4A, various TLR-related genes were robustly altered in AMs after exposure to the stimulated BALF EVs in vivo. Interestingly, the patterns of gene expression were significantly different from mice that were exposed to noninfectious EVs and to infectious EVs (Fig. 4A). More importantly, the patterns of TLR expression in AMs were significantly different between the noninfectious EV-treated (hyperoxia and acid) groups and the infectious EV-stimulated (LPS, *P. pneumonia*, and *S. pneumonia*) groups (Fig. 4B). Significant induction of TLR2 and reduction of TLR8 was observed in macrophages exposed to the EVs obtained after noninfectious stimuli. In contrast, all the infectious stimuli–derived EVs dramatically upregulated TLR6 in AMs in vivo (Fig. 4B). We also found that EV-containing TLR2 and TLR6 were negligible and not inducible in response to noxious stimuli (Supplemental Fig. 1C); they were also not detectable using qPCR in the purified EVs (Table II, Supplemental Fig. 1D), indicating that the ALI EV-induced TLRs do not come directly from instilled EVs. Myd88 and TRADD are key mediators for TLR-mediated and TNFR-mediated inflammatory signaling pathways, respectively (37, 38). We found that Myd88 was highly upregulated by EVs derived from mice exposed to hyperoxia, acid, LPS, or G^- bacteria (*P. pneumonia*) (Fig. 4C). Interestingly, EVs obtained from G^+ bacteria–treated (*S. pneumonia*) mice failed to upregulate Myd88 (Fig. 4C). TRADD expression was relatively stable after exposure to stimulated BALF EVs (Fig. 4C). CD80/86 are essential for macrophage activation and communication with other adaptive immune cells (39–41). We found that CD80 was dramatically upregulated by the EVs derived after infectious stimuli (Fig. 4D), whereas Gram-positive bacteria–induced EVs only triggered CD86 gene expression in AMs in vivo (Fig. 4D).

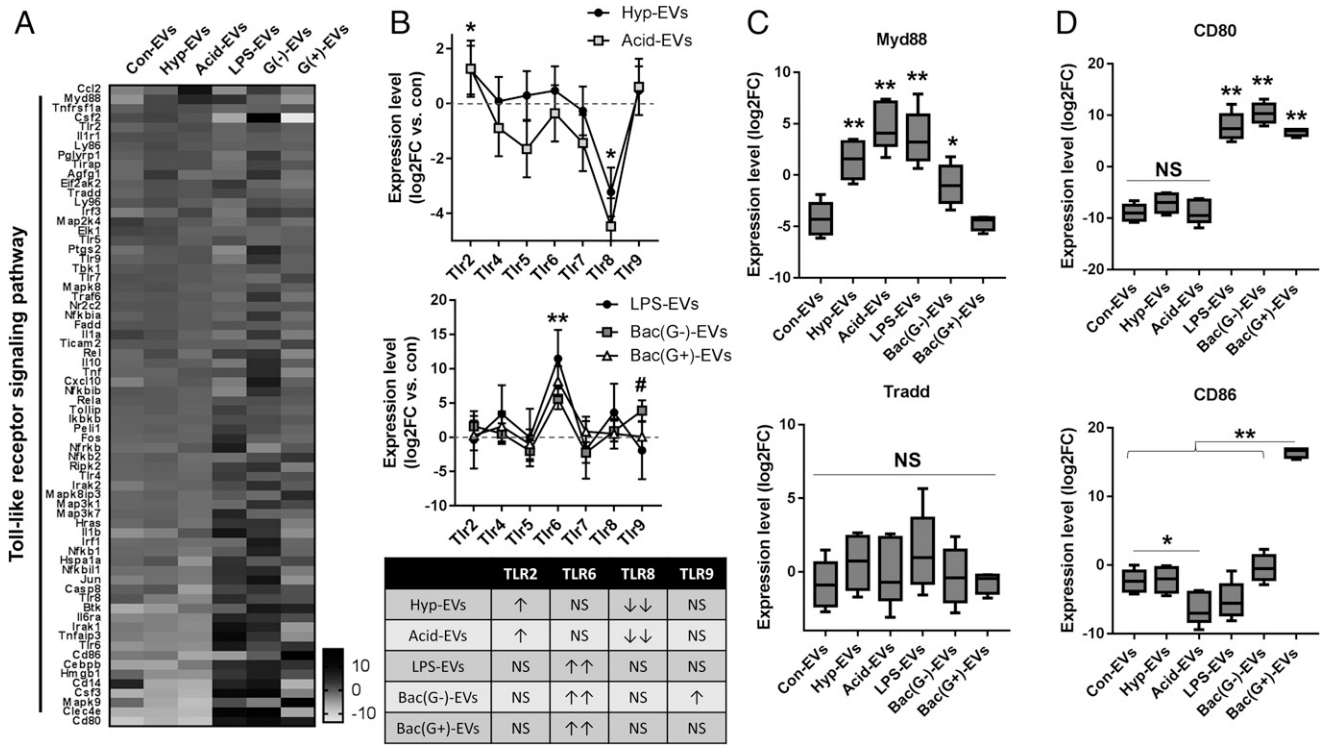

	TLR2	TLR6	TLR8	TLR9
Hyp-EVs	↑	NS	↓↓	NS
Acid-EVs	↑	NS	↓↓	NS
LPS-EVs	NS	↑↑	NS	NS
Bac(G-)-EVs	NS	↑↑	NS	↑
Bac(G+)-EVs	NS	↑↑	NS	NS

FIGURE 4. BALF EVs derived from noninfectious and infectious ALIs differentially regulate inflammatory signaling pathways in recipient AMs. BALF EVs, isolated from mice treated with hyperoxia, acid, LPS, *P. pneumoniae* (G^-), or *S. pneumoniae* (G^+) were administrated intratracheally to WT mouse lung (20 μg of EVs per mouse). After 1 d, AMs were collected and analyzed by mTOR Signaling PCR Array. Heatmap for the gene expression (**A**), TLR expression patterns and the summarized table (**B**), and expression levels of key inflammatory mediators (**C** and **D**) are shown (mean ± SD or box and whisker plot, $n = 4$ mice per group). $^*p < 0.05$, $^{**}p < 0.01$, and $^{\#}p < 0.05$ between Bac (G^-)–EVs and control.

Lung epithelial EVs or AM EVs are responsible for the development of lung inflammation after sterile and infectious stimuli, respectively

EVs were isolated from AECI and AMs after exposure of mice to noninfectious (hyperoxia) and infectious (*P. pneumonia* and *S. pneumonia*) stimuli, respectively. No bacteria were detected in the purified EVs. As shown in Fig. 5A, Con-EVs, Hyp-EVs, Bac (G^-)–EVs, or Bac (G^+)–EVs were intratracheally instilled into the recipient mouse lung. One day after instillation, BALF AMs were collected and analyzed for inflammatory gene expressions. Hyperoxia-induced epithelial EVs upregulated TLR2, Myd88, TNF-α, and IL-6 expression in recipient AMs (Fig. 5B–D) but suppressed TLR8 (Fig. 5B) in recipient AMs. Notably, the macrophage EVs derived after hyperoxia failed to alter inflammatory gene expression (Fig. 5B–D). TLR6, TLR9, CD80, IL-1β, and IL-10 were significantly upregulated in recipient AMs after exposure to AM EVs collected after exposure of mice to infectious stimuli (Fig. 5B–D). In contrast, when treated with epithelial EVs collected after exposure to infectious stimuli, IL-6 and IL-10 expression was suppressed in recipient AMs (Fig. 5C). Furthermore, TLR9 and Myd88 were only upregulated by *P. pneumonia* (G^-) infection–induced EVs, but not by EVs induced following *S. pneumonia* (G^+) infection (Figs. 4B, 4D, 5B, 5D). An overview of the proposed mechanisms of EV function in ALIs is shown (Fig. 6).

Discussion

Inflammation is a key response shared by sterile and infectious stimuli–induced ARDS/ALI (14). However, the mechanisms by which lung inflammation develops remain incompletely explored, particularly in the setting of sterile ALI. The first significant aspect of studies described in this manuscript is that we identified two distinct pathways of intercellular communication which promote the development of lung inflammation. Thus, whereas sterile

Table II. Sequence of primers used in real-time qPCR

Name	Forward Primer	Reverse Primer
TLR2	5′-GCAAACGCTGTTCTGCTCAG-3′	5′-AGGCGTCTCCCTCTATTGTATT-3′
TLR4	5′-ATGGCATGGCTTACACCACC-3′	5′-GAGGCCAATTTTGTCTCCACA-3′
TLR6	5′-TGAGCCAAGACAGAAAACCCA-3′	5′-GGGACATGAGTAAGGTTCCTGTT-3′
TLR8	5′-GGCACA ACTCCCTTGTGA-3′	5′-GCAAACGCTGTTCTGCTCAG-3′
TLR9	5′-CCGCAAGACTCTATTTGTGCTGG-3′	5′-TGTCCCTAGTCAGGGCTGTACTCAG-3′
TNF-α	5′-GACGTGGAACTGGCAGAAGAG-3′	5′-TTGGTGGTTTGTGAGTGTGAG-3′
IL-1β	5′-GCAACTGTTCCTGAACTCAACT-3′	5′-ATCTTTTGGGGTCCGTCAACT-3′
IL-6	5′-GTGACAACCACGGCCTTCCCTACT-3′	5′-GGTAGCTATGGTACTCCA-3′
IL-10	5′-GCTCTTACTGACTGGCATGAG-3′	5′-CGCAGCTCTAGGAGCATGTG-3′
Myd88	5′-TCATGTTCTCCATACCCTTGGT-3′	5′-AAACTGCGAGTGGGGTCAG-3′
CD80	5′-CTGGGAAAAACCCCCAGAAG-3′	5′-TGACAACGATGACGACGACTG-3′

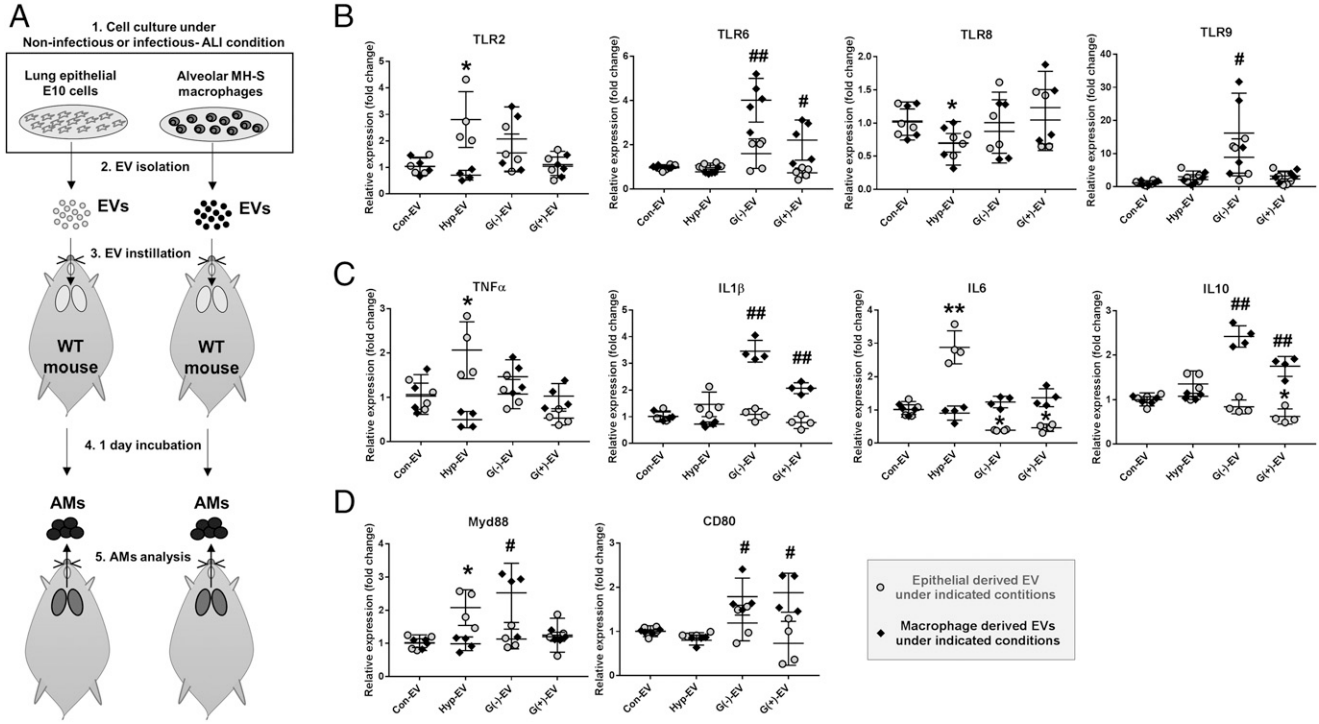

FIGURE 5. Epithelial EVs and macrophage EVs differently contribute to lung inflammation in noninfectious and infectious ALI conditions. EVs were isolated from lung alveolar epithelial type I (E10) cells and AMs (MH-S) under noninfectious (hyperoxia exposure) and infectious (*P. pneumonia* or *S. pneumonia* administration) stimuli. The isolated EVs were intratracheally delivered into WT mouse lung (20 μg of EVs per mouse). One day later, AMs were isolated from the mouse BALF as illustrated in (**A**). Gene expression levels of TLRs (**B**), cytokines (**C**), and inflammatory mediators (**D**) were evaluated from the isolated AMs. (mean ± SD, n = 4–5 per group). $^{*}p < 0.05$, $^{**}p < 0.01$, $^{\#}p < 0.05$, and $^{\#\#}p < 0.01$.

stimuli–induced EVs are mainly derived from lung epithelial cells, and uptake of epithelial EVs facilitates AM classical activation (M1), infectious stimuli mainly act on AMs stimulating the release of EVs into BALF, propagating AM classical activation. This observation is consistent with previous reports showing that noninfectious stimuli first target lung epithelium (42). AMs, as the first arm of host defense in the respiratory track, play crucial roles in the elimination of inhaled bacteria, as well as the transmission and amplification of inflammatory signals (43). Following bacterial infection, AMs are activated toward a proinflammatory phenotype (classical or M1 activation) and acquire an enhanced capacity to engulf bacteria and release inflammatory cytokines/chemokines, as well as reactive oxygen and nitrogen species (44). AM-released EVs facilitate the communication between activated AMs and resting AMs, subsequently propagating the inflammatory cascade. Our observations regarding BALF EV release in the infectious models confirm that AMs indeed are the initial responders upon encountering inhaled microbes.

In our studies, we mainly focused on the transportation of EVs from lung epithelial cells to AMs (sterile model) or from AMs to adjacent AMs (infectious model). The reverse direction of EV transfer (i.e., from AMs to epithelial cells) certainly exists (45). However, in the presence of sterile stimuli, AECI are the first responders and the EVs released from AECI are increased the most robustly. Therefore, we did not address the reverse transportation of AM-derived EVs to lung epithelial cells in the presence of sterile stimuli. In the setting of infectious models, AM-derived EVs not only were transferred to adjacent AMs, but also transferred to lung epithelial cells as we previously reported (45). The adjacent AMs engulf many more AM-derived EVs via phagocytosis or lipid raft–mediated endocytosis (46, 47). Epithelial cells may only take AM-derived EVs via the lipid raft–mediated endocytosis (47) or alternatively, receive the EV-transmitted information via surface Ag–associated signaling transduction (48).

Another important finding in this study is that in both the sterile and infectious models, the vast majority of BALF EVs fell into the range of MVs rather than Exos or ABs. As described above, ABs, MVs, and Exos have distinct mechanisms of generation (5, 6). The different routes of EV generation contribute to the different compositions of each type of EV, subsequently leading to differential biological functions (3, 5). For example, unlike the MVs, Exos have been reported to carry minimal amounts of microRNAs (miRNAs). Less than one copy of miRNA per Exo has been reported (49). In contrast to Exos, MV-containing RNA molecules, rather than MV-proteins, are the main compositions that are altered the most significantly (3). Therefore, in each disease model, identification of the precise type of EVs (i.e., MVs or Exos) is important for the development of potential therapeutic strategies targeting functional EV compositions. To our knowledge, our current report, for the first time, delineated the three different categories of EVs in each ALI models.

Probably the most significant observation in this study is that BALF EVs generated in either the noninfectious or infectious ALI models regulated AM-mediated inflammatory lung responses. Despite the fact that the stimuli-induced BALF EVs originated from different cells, AECI versus AMs, in sterile or infectious models, the recipient cells of the stimuli-induced EVs were AMs in both types of models. This observation indicates that EVs, particularly MVs, serve as a vehicle to transport the "stress" signals from the first encounters to AMs to initiate or propagate inflammatory responses. Cytokines, chemokines, and other well-known molecules have been shown to facilitate proinflammatory signal transduction (50) in the setting of ALI/ARDS (51, 52). However, many details remain unclear. For instance, how are cytokines/chemokines guided to the correct recipient cells (such as AMs)? How do AMs maintain concentrations of cytokines/chemokines during their journey from the first cells they encounter to recipient cells? Our studies provide novel insights

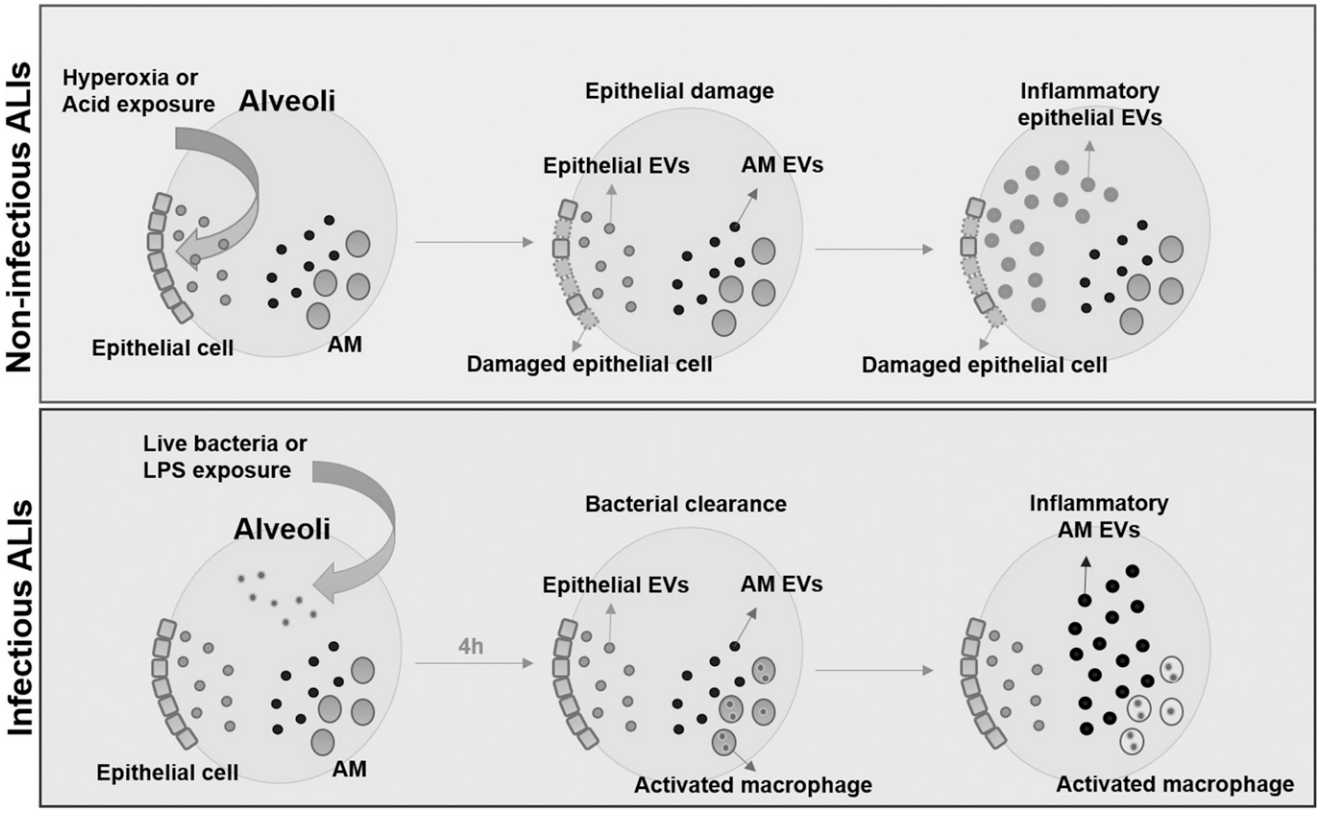

FIGURE 6. Proposed mechanisms of EV function in ALIs. Under noninfectious conditions, such as hyperoxia and acid exposure, lung epithelial cells are the first cells to actively produce EVs. These epithelial EVs contribute to the development of inflammatory lung responses by activating AMs. Conversely, after bacterial infections, AMs are the first defender and main immune cells in the lung. AMs generate proinflammatory EVs and propagate lung inflammation.

into these questions. EVs potentially serve as a carrier or vehicle to transport signaling molecules. They also maintain the necessary concentration and structure of the signaling molecules, as well as protect EV cargo from enzymatic degradation. Previous studies showed that EV-containing miRNAs are essential in promoting lung inflammation in various models of ALI (3, 30). miRNAs are small, non-coding RNA molecules (21–23 nt) involved in transcriptional and posttranscriptional regulation of gene expression (53). We demonstrated that EV-containing miR-17, 221, and 320a are upregulated in ALI and stimulate the macrophage recruitment, inflammatory signaling, cytokine production, and MMP-9 secretion in recipient macrophages (3, 30). The present studies demonstrate that soluble factors (non–EV-shuttling molecules) likewise contribute to inflammatory lung responses during the development of ALI. Therefore, both BALF EVs and BALF soluble factors are most likely keys to the pathogenesis of dysregulated lung inflammation in ALI/ARDS.

The present studies also delineated differences of EV-mediated signal transduction in the process of classic macrophage activation. In recipient AMs, we found that TLR2, IL-6, TNF-α, and Myd88 are significantly upregulated by sterile stimuli–induced BALF EVs. Similar results were obtained in macrophages after treatment with stimuli-induced lung epithelial EVs. In contrast, infectious stimuli–induced BALF EVs and AM EVs are responsible for the induction of TLR6, IL-1β, IL-10, and CD80 in the recipient AMs. Interestingly, TLR9 and Myd88 are only upregulated by EVs obtained after G^- bacterial infection, but not by EVs induced by G^+ bacteria. These results confirmed the involvement of TLR pathways in EV-mediated macrophage activation; however, this occurs by different TLR receptors and signaling cascades. Both TLR2 and TLR6 are important receptors for NF-κB–mediated inflammation in various lung diseases (54). Although expression of TLR2 is important for activation of AMs in noninfectious models (55), TLR6 expression is essential for recognition and discrimination of various bacterial lipoproteins (56, 57). Taken together, our observations suggest that lung epithelial EV–mediated TLR2 upregulation and macrophage EV–mediated TLR6 induction play central roles in the pathogenesis of lung inflammation in the setting of sterile and infectious ALI, respectively. Additionally, TLR9 is only induced by G^- bacteria–induced EVs and is LPS-independent (Fig. 4B). CD80 and CD86 belong to the B7 family and act as macrophage activators (40, 41). In our studies, CD80 and CD86 were differentially regulated by G^- bacteria–induced EVs and G^+ bacteria–induced EVs, supporting the complexity of EV-mediated signaling pathways.

One of the potential concerns in this report is that in the setting of bacterial infections, BALF EVs contain not only EVs derived from host cells but also bacteria-generated OMVs. The size of OMVs is approximately the same as the Exos (32). In our studies, we used ultra-centrifugation and filtration (0.45-μm pore size) to isolate MVs and Exos. We confirmed the sizes of EVs using DLS and NTA, as well as TEM. To further analyze the purity of BALF EVs, we evaluated the expression of bacterial OMV marker (bacterial OMP) in the BALF EVs. Bacterial OMP was not detectable in the purified BALF EVs after bacteria instillation (up to 10^8 CFU), suggesting that OMVs do not exist or are undetectable in our purified BALF EVs.

A second concern is that the functional effects of BALF EVs may result from non-physiological and excess amount of EVs used in functional studies. To limit this potential problem, we first isolated

BALF MVs from one mouse. Next, we instilled the single mouse-derived MVs into the recipient mouse in a 1:1 ratio.

During the processes of EV isolation using sequential centrifugation, several critical steps required attention. First, it is best if EV isolation is performed immediately after BALF is collected. We observed significant EV aggregation and size alteration when EVs are isolated using the frozen BALF. It is presumably difficult to recover the original character of EVs after freezing. Second, we recommend a soft sonication of the isolated EVs using a water-bath sonicator before the EV NTA or functional assays are performed. The soft sonication effectively disperses the EV aggregates, which are possibly generated during the sequential centrifugation or freeze/thaw step. This step significantly contributes to consistency of the obtained results. Third, we do not recommend a long-term storage of the isolated EVs. We noted a remarkable destruction of EV components, such as proteins and RNAs, after the long-term storage of the EVs.

Collectively, to our knowledge, the current study provides the first evidence that sterile and infectious stimuli–induced MVs were differentially generated in vivo. Despite the diverse sources of EVs, both sterile stimuli–induced EVs and infection-induced EVs facilitated classic AM activation and subsequently promoted inflammatory lung responses via different signaling pathways. Based on our observation, noninfectious ALI models would be suitable for EV research focusing on lung epithelial cells, whereas the infectious ALI models are probably better to study BALF EVs derived from AMs or other immunomodulatory cells, as proposed in Fig. 6. Our results potentially provide novel insights into the role of EVs research in ALI and experimental strategies using various ALI models.

Acknowledgments

We thank Dr. Bruce Levy (Pulmonary and Critical Care Medicine, Brigham and Women's Hospital, Boston, MA) and the rest of the laboratory for information and education on the acid inhalation–induced lung injury model.

Disclosures

The authors have no financial conflicts of interest.

References

1. Tkach, M., and C. Théry. 2016. Communication by extracellular vesicles: where we are and where we need to go. *Cell* 164: 1226–1232.
2. Chargaff, E., and R. West. 1946. The biological significance of the thromboplastic protein of blood. *J. Biol. Chem.* 166: 189–197.
3. Lee, H., D. Zhang, Z. Zhu, C. S. Dela Cruz, and Y. Jin. 2016. Epithelial cell-derived microvesicles activate macrophages and promote inflammation via microvesicle-containing microRNAs. *Sci. Rep.* 6: 35250.
4. Moldovan, L., K. Batte, Y. Wang, J. Wisler, and M. Piper. 2013. Analyzing the circulating microRNAs in exosomes/extracellular vesicles from serum or plasma by qRT-PCR. *Methods Mol. Biol.* 1024: 129–145.
5. Crescitelli, R., C. Lässer, T. G. Szabó, A. Kittel, M. Eldh, I. Dianzani, E. I. Buzás, and J. Lötvall. 2013. Distinct RNA profiles in subpopulations of extracellular vesicles: apoptotic bodies, microvesicles and exosomes. *J. Extracell. Vesicles* Available at: https://doi.org/10.3402/jev.v2i0.20677.
6. Turturici, G., R. Tinnirello, G. Sconzo, and F. Geraci. 2014. Extracellular membrane vesicles as a mechanism of cell-to-cell communication: advantages and disadvantages. *Am. J. Physiol. Cell Physiol.* 306: C621–C633.
7. Campanella, C., F. Bucchieri, A. M. Merendino, A. Fucarino, G. Burgio, D. F. Corona, G. Barbieri, S. David, F. Farina, G. Zummo, et al. 2012. The odyssey of Hsp60 from tumor cells to other destinations includes plasma membrane-associated stages and Golgi and exosomal protein-trafficking modalities. *PLoS One* 7: e42008.
8. Johnstone, R. M., M. Adam, J. R. Hammond, L. Orr, and C. Turbide. 1987. Vesicle formation during reticulocyte maturation. Association of plasma membrane activities with released vesicles (exosomes). *J. Biol. Chem.* 262: 9412–9420.
9. Ng, Y. H., S. Rome, A. Jalabert, A. Forterre, H. Singh, C. L. Hincks, and L. A. Salamonsen. 2013. Endometrial exosomes/microvesicles in the uterine microenvironment: a new paradigm for embryo-endometrial cross talk at implantation. *PLoS One* 8: e58502.
10. Dalli, J., L. V. Norling, D. Renshaw, D. Cooper, K. Y. Leung, and M. Perretti. 2008. Annexin 1 mediates the rapid anti-inflammatory effects of neutrophil-derived microparticles. *Blood* 112: 2512–2519.
11. Gulinelli, S., E. Salaro, M. Vuerich, D. Bozzato, C. Pizzirani, G. Bolognesi, M. Idzko, F. Di Virgilio, and D. Ferrari. 2012. IL-18 associates to microvesicles shed from human macrophages by a LPS/TLR-4 independent mechanism in response to P2X receptor stimulation. *Eur. J. Immunol.* 42: 3334–3345.
12. Atkin-Smith, G. K., S. Paone, D. J. Zanker, M. Duan, T. K. Phan, W. Chen, M. D. Hulett, and I. K. Poon. 2017. Isolation of cell type-specific apoptotic bodies by fluorescence-activated cell sorting. *Sci. Rep.* 7: 39846.
13. Suchorska, W. M., and M. S. Lach. 2016. The role of exosomes in tumor progression and metastasis (Review). *Oncol. Rep.* 35: 1237–1244.
14. Matute-Bello, G., C. W. Frevert, and T. R. Martin. 2008. Animal models of acute lung injury. *Am. J. Physiol. Lung Cell. Mol. Physiol.* 295: L379–L399.
15. McVey, M., A. Tabuchi, and W. M. Kuebler. 2012. Microparticles and acute lung injury. *Am. J. Physiol. Lung Cell. Mol. Physiol.* 303: L364–L381.
16. Yamamoto, K., J. D. Ferrari, Y. Cao, M. I. Ramirez, M. R. Jones, L. J. Quinton, and J. P. Mizgerd. 2012. Type I alveolar epithelial cells mount innate immune responses during pneumococcal pneumonia. *J. Immunol.* 189: 2450–2459.
17. Jin, Y., H. P. Kim, J. Cao, M. Zhang, E. Ifedigbo, and A. M. Choi. 2009. Caveolin-1 regulates the secretion and cytoprotection of Cyr61 in hyperoxic cell death. *FASEB J.* 23: 341–350.
18. Bhatnagar, S., K. Shinagawa, F. J. Castellino, and J. S. Schorey. 2007. Exosomes released from macrophages infected with intracellular pathogens stimulate a proinflammatory response in vitro and in vivo. *Blood* 110: 3234–3244.
19. Bateman, S. L., and P. Seed. 2012. Intracellular macrophage infections with *E. coli* under nitrosative stress. *Bio Protoc.* 2: e275. Available at: https://doi.org/10.21769/BioProtoc.275.
20. Moon, H. G., Y. Cao, J. Yang, J. H. Lee, H. S. Choi, and Y. Jin. 2015. Lung epithelial cell-derived extracellular vesicles activate macrophage-mediated inflammatory responses via ROCK1 pathway. *Cell Death Dis.* 6: e2016.
21. Traber, K. E., K. L. Hilliard, E. Allen, G. A. Wasserman, K. Yamamoto, M. R. Jones, J. P. Mizgerd, and L. J. Quinton. 2015. Induction of STAT3-dependent CXCL5 expression and neutrophil recruitment by oncostatin-M during pneumonia. *Am. J. Respir. Cell Mol. Biol.* 53: 479–488.
22. Atkin-Smith, G. K., R. Tixeira, S. Paone, S. Mathivanan, C. Collins, M. Liem, K. J. Goodall, K. S. Ravichandran, M. D. Hulett, and I. K. Poon. 2015. A novel mechanism of generating extracellular vesicles during apoptosis via a beads-on-a-string membrane structure. *Nat. Commun.* 6: 7439.
23. Clancy, J. W., A. Sedgwick, C. Rosse, V. Muralidharan-Chari, G. Raposo, M. Method, P. Chavrier, and C. D'Souza-Schorey. 2015. Regulated delivery of molecular cargo to invasive tumour-derived microvesicles. *Nat. Commun.* 6: 6919.
24. Zhang, H. M., Q. Li, X. Zhu, W. Liu, H. Hu, T. Liu, F. Cheng, Y. You, Z. Zhong, P. Zou, et al. 2016. miR-146b-5p within BCR-ABL1-positive microvesicles promotes leukemic transformation of hematopoietic cells. *Cancer Res.* 76: 2901–2911.
25. Lee, H. D., Y. H. Kim, and D. S. Kim. 2014. Exosomes derived from human macrophages suppress endothelial cell migration by controlling integrin trafficking. *Eur. J. Immunol.* 44: 1156–1169.
26. Dye, B. R., D. R. Hill, M. A. Ferguson, Y. H. Tsai, M. S. Nagy, R. Dyal, J. M. Wells, C. N. Mayhew, R. Nattiv, O. D. Klein, et al. 2015. In vitro generation of human pluripotent stem cell derived lung organoids. *Elife* 4: e05098.
27. Fehrenbach, H., G. Zissel, T. Goldmann, T. Tschernig, E. Vollmer, R. Pabst, and J. Müller-Quernheim. 2003. Alveolar macrophages are the main source for tumour necrosis factor-alpha in patients with sarcoidosis. *Eur. Respir. J.* 21: 421–428.
28. Gauna, A. E., and S. Cha. 2014. Akt2 deficiency as a therapeutic strategy protects against acute lung injury. *Immunotherapy* 6: 377–380.
29. Zhang, X., R. Goncalves, and D. M. Mosser. 2008. The isolation and characterization of murine macrophages. *Curr Protoc Immunol* Chapter 14: Unit 14.1.
30. Lee, H., D. Zhang, J. Wu, L. E. Otterbein, and Y. Jin. 2017. Lung epithelial cell-derived microvesicles regulate macrophage migration via microRNA-17/221-induced integrin β_1 recycling. *J. Immunol.* 199: 1453–1464.
31. Xu, R., D. W. Greening, A. Rai, H. Ji, and R. J. Simpson. 2015. Highly-purified exosomes and shed microvesicles isolated from the human colon cancer cell line LIM1863 by sequential centrifugal ultrafiltration are biochemically and functionally distinct. *Methods* 87: 11–25.
32. Klimentová, J., and J. Stulík. 2015. Methods of isolation and purification of outer membrane vesicles from gram-negative bacteria. *Microbiol. Res.* 170: 1–9.
33. Jay, S. J., W. G. Johanson, Jr., A. K. Pierce, and J. S. Reisch. 1976. Determinants of lung bacterial clearance in normal mice. *J. Clin. Invest.* 57: 811–817.
34. Jain-Vora, S., A. M. LeVine, Z. Chroneos, G. F. Ross, W. M. Hull, and J. A. Whitsett. 1998. Interleukin-4 enhances pulmonary clearance of *Pseudomonas aeruginosa*. *Infect. Immun.* 66: 4229–4236.
35. Matzer, S. P., T. Baumann, N. W. Lukacs, M. Röllinghoff, and H. U. Beuscher. 2001. Constitutive expression of macrophage-inflammatory protein 2 (MIP-2) mRNA in bone marrow gives rise to peripheral neutrophils with preformed MIP-2 protein. *J. Immunol.* 167: 4635–4643.
36. Goldstein, E., W. Lippert, and D. Warshauer. 1974. Pulmonary alveolar macrophage. Defender against bacterial infection of the lung. *J. Clin. Invest.* 54: 519–528.
37. Warner, N., and G. Núñez. 2013. MyD88: a critical adaptor protein in innate immunity signal transduction. [Published erratum appears in 2013 *J. Immunol.* 190: 3824.] *J. Immunol.* 190: 3–4.
38. Ermolaeva, M. A., M. C. Michallet, N. Papadopoulou, O. Utermöhlen, K. Kranidioti, G. Kollias, J. Tschopp, and M. Pasparakis. 2008. Function of

TRADD in tumor necrosis factor receptor 1 signaling and in TRIF-dependent inflammatory responses. *Nat. Immunol.* 9: 1037–1046.
39. Nolan, A., H. Kobayashi, B. Naveed, A. Kelly, Y. Hoshino, S. Hoshino, M. R. Karulf, W. N. Rom, M. D. Weiden, and J. A. Gold. 2009. Differential role for CD80 and CD86 in the regulation of the innate immune response in murine polymicrobial sepsis. *PLoS One* 4: e6600.
40. Liu, M. F., J. S. Li, T. H. Weng, and H. Y. Lei. 1999. Differential expression and modulation of costimulatory molecules CD80 and CD86 on monocytes from patients with systemic lupus erythematosus. *Scand. J. Immunol.* 49: 82–87.
41. Creery, W. D., F. Diaz-Mitoma, L. Filion, and A. Kumar. 1996. Differential modulation of B7-1 and B7-2 isoform expression on human monocytes by cytokines which influence the development of T helper cell phenotype. *Eur. J. Immunol.* 26: 1273–1277.
42. Modelska, K., J. F. Pittet, H. G. Folkesson, V. Courtney Broaddus, and M. A. Matthay. 1999. Acid-induced lung injury. Protective effect of anti-interleukin-8 pretreatment on alveolar epithelial barrier function in rabbits. *Am. J. Respir. Crit. Care Med.* 160: 1450–1456.
43. Kopf, M., C. Schneider, and S. P. Nobs. 2015. The development and function of lung-resident macrophages and dendritic cells. *Nat. Immunol.* 16: 36–44.
44. Arango Duque, G., and A. Descoteaux. 2014. Macrophage cytokines: involvement in immunity and infectious diseases. *Front. Immunol.* 5: 491.
45. Zhu, Z., D. Zhang, H. Lee, A. A. Menon, J. Wu, K. Hu, and Y. Jin. 2017. Macrophage-derived apoptotic bodies promote the proliferation of the recipient cells via shuttling microRNA-221/222. *J. Leukoc. Biol.* 101: 1349–1359.
46. Feng, D., W. L. Zhao, Y. Y. Ye, X. C. Bai, R. Q. Liu, L. F. Chang, Q. Zhou, and S. F. Sui. 2010. Cellular internalization of exosomes occurs through phagocytosis. *Traffic* 11: 675–687.
47. Mulcahy, L. A., R. C. Pink, and D. R. Carter. 2014. Routes and mechanisms of extracellular vesicle uptake. *J. Extracell. Vesicles* 3.
48. Urbanelli, L., A. Magini, S. Buratta, A. Brozzi, K. Sagini, A. Polchi, B. Tancini, and C. Emiliani. 2013. Signaling pathways in exosomes biogenesis, secretion and fate. *Genes (Basel)* 4: 152–170.
49. Chevillet, J. R., Q. Kang, I. K. Ruf, H. A. Briggs, L. N. Vojtech, S. M. Hughes, H. H. Cheng, J. D. Arroyo, E. K. Meredith, E. N. Gallichotte, et al. 2014. Quantitative and stoichiometric analysis of the microRNA content of exosomes. *Proc. Natl. Acad. Sci. USA* 111: 14888–14893.
50. Turner, M. D., B. Nedjai, T. Hurst, and D. J. Pennington. 2014. Cytokines and chemokines: at the crossroads of cell signalling and inflammatory disease. *Biochim. Biophys. Acta* 1843: 2563–2582.
51. Puneet, P., S. Moochhala, and M. Bhatia. 2005. Chemokines in acute respiratory distress syndrome. *Am. J. Physiol. Lung Cell. Mol. Physiol.* 288: L3–L15.
52. Goodman, R. B., J. Pugin, J. S. Lee, and M. A. Matthay. 2003. Cytokine-mediated inflammation in acute lung injury. *Cytokine Growth Factor Rev.* 14: 523–535.
53. Ha, M., and V. N. Kim. 2014. Regulation of microRNA biogenesis. *Nat. Rev. Mol. Cell Biol.* 15: 509–524.
54. Lafferty, E. I., S. T. Qureshi, and M. Schnare. 2010. The role of toll-like receptors in acute and chronic lung inflammation. *J. Inflamm. (Lond.)* 7: 57.
55. Jiang, D., J. Liang, Y. Li, and P. W. Noble. 2006. The role of Toll-like receptors in non-infectious lung injury. *Cell Res.* 16: 693–701.
56. Kang, J. Y., X. Nan, M. S. Jin, S. J. Youn, Y. H. Ryu, S. Mah, S. H. Han, H. Lee, S. G. Paik, and J. O. Lee. 2009. Recognition of lipopeptide patterns by Toll-like receptor 2-Toll-like receptor 6 heterodimer. *Immunity* 31: 873–884.
57. Takeuchi, O., T. Kawai, P. F. Mühlradt, M. Morr, J. D. Radolf, A. Zychlinsky, K. Takeda, and S. Akira. 2001. Discrimination of bacterial lipoproteins by Toll-like receptor 6. *Int. Immunol.* 13: 933–940.